Journal of Metals, Materials and Minerals, 34(1), 1931, 2024

Green synthesis of bimetallic CuO@NiO nanocomposite for the removal of glyphosate

Kornkanok BOONSERM[1], Anan SUTCHA[2], and Rarm PHINJAROENPHAN[2,*]

[1] *Department of Applied Chemistry, Faculty of Sciences and Liberal Arts, Rajamangala University of Technology Isan, 744, Suranarai Road, Muang District, Nakhon Ratchasima 30000, Thailand*

[2] *Department of Applied Physics, Faculty of Sciences and Liberal Arts, Rajamangala University of Technology Isan, 744, Suranarai Road, Muang District, Nakhon Ratchasima 30000, Thailand*

***Corresponding author e-mail**: rarm.ph@rmuti.ac.th

Received date:
13 January 2024
Revised date
13 February 2024
Accepted date:
12 March 2024

Keywords:
CuO@NiO nanocomposite;
Mango peel;
Mangifera indica L;
Glyphosate;
Photocatalytic activity

Abstract

Green synthesis of photocatalyst bimetallic CuO@NiO nanocomposite for eliminating organic hazardous glyphosate (Gly) solution has been introduced. The nanocomposite has been successfully developed from mango (*Mangifera indica L.*) peel extracted solution by a simultaneous reduction process. HRTEM, XRD, and EDX have also been used to explore the nanostructure, crystal conformation, and chemical compositions of CuO@NiO. Using UV-vis spectrometer, we have observed the photocatalytic activity and kinetic removal rate constant of CuO@NiO in terms of glyphosate elimination under UV light illumination. Compared with pure CuO and NiO nanoparticles, CuO@NiO displayed improved and enhanced photocatalytic activity. This work demonstrates an eco-friendly, low-cost material with high efficiency for removing Gly, which has applications in environmental protection.

1. Introduction

Recently, water pollution problems from the contamination of herbicides have been seriously a concern. The high demand for agricultural production, thereby increases the use of herbicides and generates wastewater from herbicide-contaminated pollution. Glyphosate is one of a kind herbicide that has been intensively and widely used in agriculture [1], because it is capable of removing broadleaf weeds and grasses to protect crops. By using glyphosate for a long time and carelessly, toxic effluent and residue from the glyphosate have negative effects on human health and other living things, as well as cause contaminated water pollution [1-3].

Many developed techniques for glyphosate removal in contaminated water have been reported based on removal methods, such as adsorption, filtration, ultrafiltration, reverse osmosis, biological degradation, and photocatalysis processes. Among these methods, photocatalysis derived much attention owing to its good efficiency in removal rate, easy to use, cost-effectiveness, and low energy consumption [4-6]. While adsorption, filtration, ultrafiltration, and reverse osmosis processes are more expensive, require some specific method for particular contaminants, and need to use large equipment [7-9]. Besides, biological processes might produce more toxic by-products if we do not control parameters during the degradation of glyphosate [9].

Bimetallic nanoparticles have been composed of two different metals and at least one of them has a structure in the nanoscale. Due to the co-existence and integrated working of the metals, it enhances and improves physical, chemical, optical, electrical, magnetic, and catalysis properties over monometallic nanoparticles. Therefore, bimetallic nanoparticles have been recently received interest from many researchers and used widely in many fields, such as catalysis [10-12], electrochemistry [13-14], magnetism [15-17], and optics [17-19], respectively.

Among the wildly potential applications of bimetallic nanoparticles, is the utilization as a photocatalyst to remove and eliminate organic toxicity waste and, consequently, prevent water pollution. The elimination of toxic waste has been attributed to generating electrons (e^-) and holes (h^+) under light exposure. The photogenerated electrons (e^-) and holes (h^+) react with O_2 and H_2O molecules and produce oxide radicals (O_2^-) and hydroxyl radicals ($OH^\cdot$), respectively. These radical oxidizing sites are strong enough to remove hazardous waste.

Recently, the eco-friendly method for preparing nanoparticles has been introduced as a green synthesis process. The green technique uses plants and fruits such as aloe vera leaf [20], mahogany leaf [21], papaya leaf [22], orange peel [23], mango peel [24], and custard apple peel [25], to create nanoparticles, so it does not use any toxic chemical substances such as reducing agents, organic solvents, and stabilizers and thus subsequently reduces environmental toxicity [26-28]. Besides, this technique is low cost, energy conservation, and may produce large-scale nanoparticles [28].

It has been reported that nanocomposite materials based on Cu and Ni systems are one of the most promising photocatalysts because of their present high photocatalytic efficiency, availability, less toxicity, and low cost [29-31]. In addition, Ramu et al. [32] have successfully

prepared CuO@NiO nanocomposite by using a hydrothermal approach. The CuO@NiO nanocomposite was found to be spherical having an average particle size around 25 nm. The synthesized CuO@NiO could eliminate toxic aromatic nitrophenols, such as NP, DNP, and TNP within 2, 5, and 10 min, with expressed very high kinetic rate constants about 1.519, 0.5102, 0.4601 min^{-1}, respectively. Another work on the composites of Cu-Ni nanocomposite has been reported by Younas *et al*. [33]. They reported that the green synthesis Cu-Ni was obtained from Gazania rigens extract, and used as a photocatalyst to eliminate organic methyl blue (MB) dye solution. The particle size of Cu-Ni was observed at around 50 nm to 100 nm and expressed high performance of removal MB dye. They showed that Cu-Ni could degrade MB within 19 min with a rate constant of 0.2505 min^{-1}. Furthermore, Abdullah *et al.* [34] developed Cu-Ni hybrid nanocomposite from Zingiber officinale rhizome extract. SEM analysis suggested that the Cu-Ni contains an irregular shape with a mean diameter of 25.12 nm ± 1.2 nm. The authors found that the green synthesis Cu-Ni was able to remove the crystal violet dye up to 95% within 160 min under UV illumination. The authors also pointed out that Cu-Ni nanocomposite gives a better rate of removing violet dye solution than the pure Cu and Ni nanoparticles.

Although the photocatalytic properties of CuO@NiO have been emerged and published, there are just a few reports on the study and discussion of CuO@NiO system for the removal of glyphosate (Gly). Hence, in this work, we presented a green development of photocatalyst CuO@NiO nanocomposite for the degradation of Gly. The CuO@NiO was synthesized from mango (*Mangifera indica L.*) peel extracted solution by a simultaneous reduction process. We believe that the fabricated photocatalyst CuO@NiO from *Mangifera indica L.* peel for the elimination of Gly has not yet been reported. The effects of various catalyst dosages and reaction time, as well as, kinetic study on Gly removal under UV light irradiation, were investigated and discussed. Not only that, the comparison of photocatalytic activity between CuO@NiO nanocomposite and pure CuO and NiO nanoparticles has also been demonstrated.

2. Materials and methods

2.1 Raw materials

The chemical reagents, such as copper nitrate ($Cu(NO_3)2.3H_2O$), nickel sulfate heptahydrate (NiSO4.6H2O), sodium hydroxide (NaOH), and hydrochloric acid (HCl), were derived from Sigma Aldrich in analytical grade and utilized without any further purification. Commercial-grade glyphosate (glyphosate-isopropyl ammonium) (Gly) was purchased from a local market in Nakhon Ratchasima, Thailand. Fresh mango (*Mangifera indica L.*) peel was collected in a fruit shop in Nakhon Ratchasima, Thailand.

2.2 Synthesis of CuO and NiO nanoparticles

The aqueous solution was extracted from mango (*Mangifera indica L.*) peel for use as a reducing agent for the synthesis of CuO, NiO, and CuO@NiO nanoparticles. The mango peel was collected and washed with distilled water to remove dust and other contaminants. Then, the samples were dried under sunlight for a day and ground into fine powder using an electric grinder. Ten grams of the peel powder was boiled with 100 mL of deionized water at 90°C with stirring for 30 min to extract reduce and capping agents such as polyphenols substances [24]. Afterward, the mango peel extracted solution was left to cool and filtered with filter paper.

CuO nanoparticle could be synthesized by mixing 10 mM copper nitrate with 40 mL of peel extract solution under constant stirring at 60°C. Then, adjusted to pH 7, and stirred for another 180 min at the same temperature. The precipitation of the CuO was obtained by using a centrifuge and washed with ethanol and deionized water several times. Subsequently, the nanoparticle was dried in an oven at 100°C for 3 h. While NiO nanoparticle was obtained by using the same method, but using 50 mM nickel sulfate instead of copper nitrate.

2.3 Synthesis of CuO@NiO nanocomposite

CuO@NiO nanocomposite was also produced by using a similar process as mentioned above, however, the difference was the presence of both CuO and NiO. In this process, 50 mM nickel sulfate was mixed with 40 mL of the mango peel extract solution under constant stirring at 60°C for 15 min. Next, 10 mM copper nitrate was added to the previous solution, adjusted to pH 7, and stirred for another 180 min. The precipitation of the CuO@NiO nanocomposite was also derived using a centrifuge and washed with ethanol and deionized water several times. Lastly, these CuO@NiO particles were dried in an oven at 100°C for 3 h.

2.4 Characterization

The X-ray diffraction (XRD) measurements were carried out using a Rigaku D/Max 2,500 X-ray diffractometer with CuKα radiation of wavelength 0.154 nm. The high- resolution transmission electron microscopy (HRTEM) was measured by a Tecnai G2 20 transmission electron microscopy. The energy dispersion X-ray spectrometer (EDS), attached to the scanning electron microscopy (SEM), was used to characterize. The EDX samples were also prepared by placing dried nanoparticles on the carbon tape. The average crystallite size can be determined from Debye–Scherrer's formula as shown in Equation (1).

$$D = \frac{k\lambda}{\beta cos\theta} \quad (1)$$

where D is the average crystalline size, k is the Sherrer constant taken as equal to 0.89, λ is the wavelength of the X-ray (0.154 nm), β is the full width at half maximum of the diffraction peak, and θ is the angular position of the diffraction peak.

2.5 Photocatalytic activity evaluation

The photocatalytic activity of all the synthesized samples, such as CuO@NiO, CuO, and NiO were performed in batch experiments at room temperature, and determined in terms of removal rates of glyphosate (Gly) by UV-Vis spectrophotometer. The effects of various catalyst dosages and reaction time were investigated. In the experiment, a specific number of each nanoparticle was dispersed in 25 mL at an initial concentration of 4,000 ppm of Gly in a solution with pH 7. The mixture solution was stirred for 30 min in the dark (to reach the

equilibrium of adsorption and/or desorption of the nanoparticles), then irradiated under UV light with a 60-W Hg lamp working as a UV light source. At a specific irradiation time, 5 mL of the combined solution was taken, centrifuged, and filtered. The photocatalytic activity was derived by calculating the Gly concentration of the filtrate with a UV-Vis spectrometer at 193 nm (This wavelength corresponds to Gly maximum absorption). In addition, the percentage of eliminate Gly under UV light (% Gly removal) and the kinetic behavior of the catalyst can be defined as shown in Equation (2) and Equation (3), respectively.

$$\text{Gly removal (\%)} = \left(\frac{C_0 - C_t}{C_0}\right) \times 100 \quad (2)$$

$$\ln\left(\frac{C_0}{C_t}\right) = kt \quad (3)$$

where $C0$ (ppm) and Ct (ppm) represent the Gly concentration at an initial time and irradiation time, respectively. In addition, k is the removed rate constant.

3. Results and discussion

The crystal structure of all the synthesized nanoparticles was analyzed by XRD method as shown in Figure 1. The diffraction peaks of NiO were observed at around 2θ = 36.52° and 44.00°, corresponding to reflection plane (111) and (200) of cubic, according to JCPDS file no. 45-1027, respectively. Pure CuO showed diffraction peaks at around 2θ = 35.31°, 39.18°, 49.34°, and 54.34°, corresponding to reflection plane (002), (111), (-202), and (020) of monoclinic, according to JCPDS file no.45-0937. Moreover, the average crystallite size of the NiO and CuO were estimated from Debye–Scherrer's equation at around 33 nm and 39 nm, respectively.

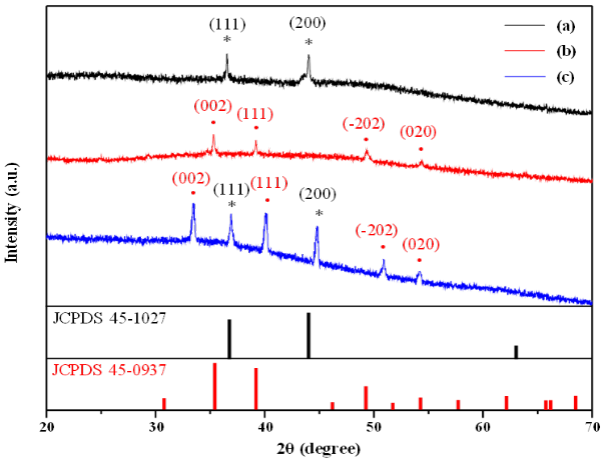

Figure 1. XRD profiles of the synthesized nanoparticles; (a) NiO, (b) CuO, and (c) CuONiO (* NiO JCPDS file no. 45-1027 • CuO JCPDS file no. 45-0937).

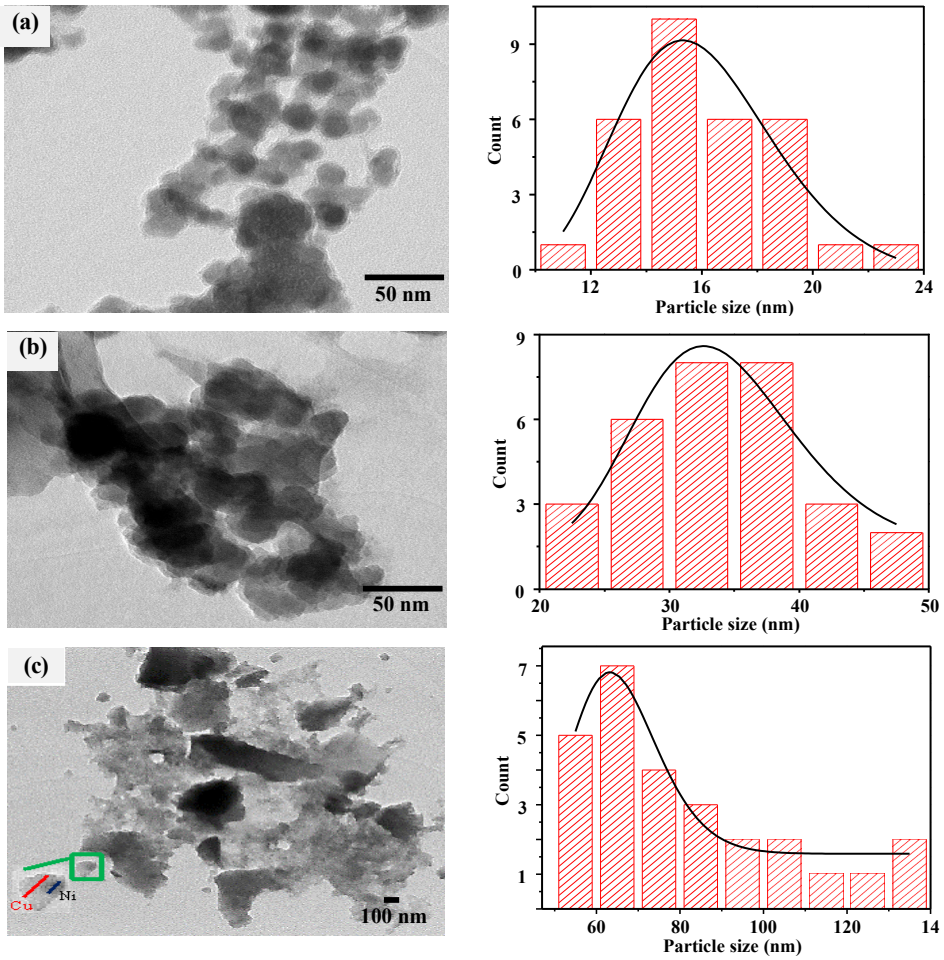

Figure 2. High-resolution TEM images and histogram of the particle size distribution of the synthesized nanoparticles: (a) NiO, (b) CuO, (c) CuONiO.

The XRD profile of the CuO@NiO was more complicated as it showed more diffraction peaks, at around 2θ = 33.46°, 36.92°, 40.09°, 44.77°, 50.89°, and 54.18°, respectively. These peaks were matched with the characteristic peaks from both monoclinic CuO (2θ = 33.46° (002), 40.09° (111), 50.89° (-202) and 54.18° (020)) and cubic NiO (2θ = 36.92° (111) and 44.77° (200)), which suggested the co-existence of CuO and NiO phases. The crystallite size of the CuO@NiO was also evaluated and obtained at about 29 nm.

The morphology and structural information of the nanoparticles were investigated by the HR-TEM technique, as shown in Figure 2. The structure of NiO was revealed to be a globular shape with an average particle size of 15.83 nm ± 0.58 nm (Figure 2(a)). CuO was also observed in spherical formation but bigger in average particle size of 33.74 nm ± 1.38 nm (Figure 2(b)), respectively. The obtained structure of CuO@NiO was a nano-subcluster (the Ni cluster was attached and shared an interface with the Cu cluster) (Figure 2(c)). The CuO@NiO was revealed in a globular conformation with a mean particle size of around 63.85 nm ± 1.26 nm. This particle size was derived larger than that value of pure CuO and NiO, as corresponding to the CuO@NiO samples were composed of the CuO and NiO.

To earn more details of the morphology information, the EDS measurements are needed to be examined. To avoid the effect of Cu from our samples, all the measurements used carbon adhesive tapes as a sample holder. According to the EDS elemental mapping results, the element of Ni was found in pure NiO (Figure 3(a)) and the element of Cu was obtained in pure CuO (Figure 3(b)), respectively. While elements of both Cu and Ni were observed from CuO@NiO products (Figure 3(c)). These results confirmed that pure NiO and CuO, as well as CuO@NiO nanocomposite, were successfully developed.

The possible mechanism of the developed CuO@NiO nanocomposite from the extracted mango peel solution could be explained by a simultaneous aqueous reduction process. Since the extract solution behaves as a mild reducing agent, it could reduce Cu and Ni ions to form nanoparticles. Besides, the reduction potential of Cu^{2+} to Cu (0.34 V) is larger than that of Ni^{2+} to Ni (−0.25 V), Cu ions can reduce and transform into Cu atoms at a faster rate than Ni atoms [11]. Therefore, at 15 min for mixing Ni ions with the solution and then followed by Cu ions, a small Ni nucleation site was formed for the Cu atoms to grow. Lastly, CuO@NiO nanoparticle subclusters were obtained. All the structural information and elemental compositions are summarized and shown in Table 1S.

The photocatalytic performance of the synthesized nanoparticles was evaluated and discussed by examining the removal rate of glyphosate (Gly) under UV light irradiation. Not only that the kinetic rate constants for the Gly removal was also determined. The experiments were carried out using 3, 6, and 9 mg of CuO@NiO added to 25 mL Gly solution at various contact times, as illustrated in Figure 4. It was found that the removal of Gly rapidly increased in the first 5 h and slightly increased afterward. More than 50% of the degradation was achieved in 5 h for all the catalyst dosages. In addition, 6 mg of CuO@NiO presented the highest removal rate of Gly up to 71.23% after 9 h. When increased to 9 mg and decreased to 3 mg of CuO@NiO, the Gly removal rate reduced to 65.30% and 60.55%, respectively, within the same time. The kinetics behavior from the CuO@NiO was found to be similar trends to their photocatalytic activity. The highest rate was 0.132 h^{-1} obtained from 6 mg of CuO@NiO, followed by 0.112 and 0.099 h^{-1} from 9 mg and 3 mg of CuO@NiO, respectively.

The results might be due to the optimized amount of CuO@NiO catalyst was 6 mg. Therefore, they gave a high among of photogenerated electrons (e^-) and hole (h^+) from UV light activation, subsequently creating a high number of radical active sites for degradation of Gly. When increasing to 9 mg of CuO@NiO, the catalyst particles were obscured and blocked UV light to activate radical sites. However, if the catalyst was reduced to 3 mg, it also reduced the number of radical sites, leading to the lowest of Gly removal rate.

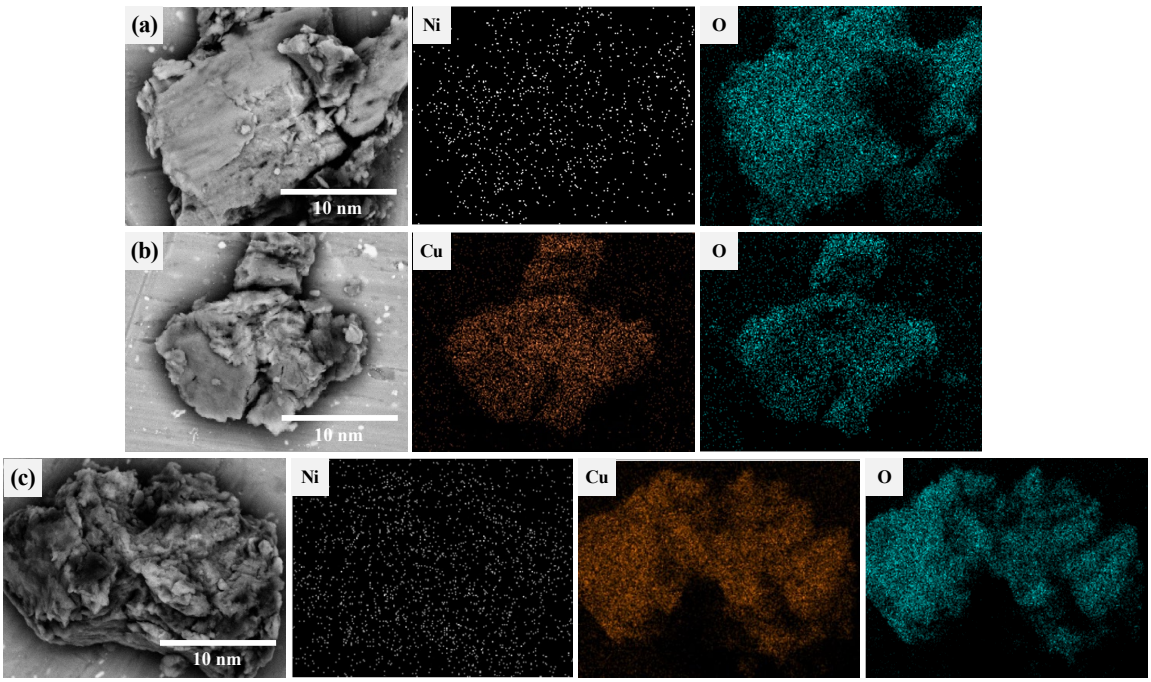

Figure 3. SEM images and EDS elemental mappings of (a) NiO, (b) CuO, and (c) CuO@NiO.

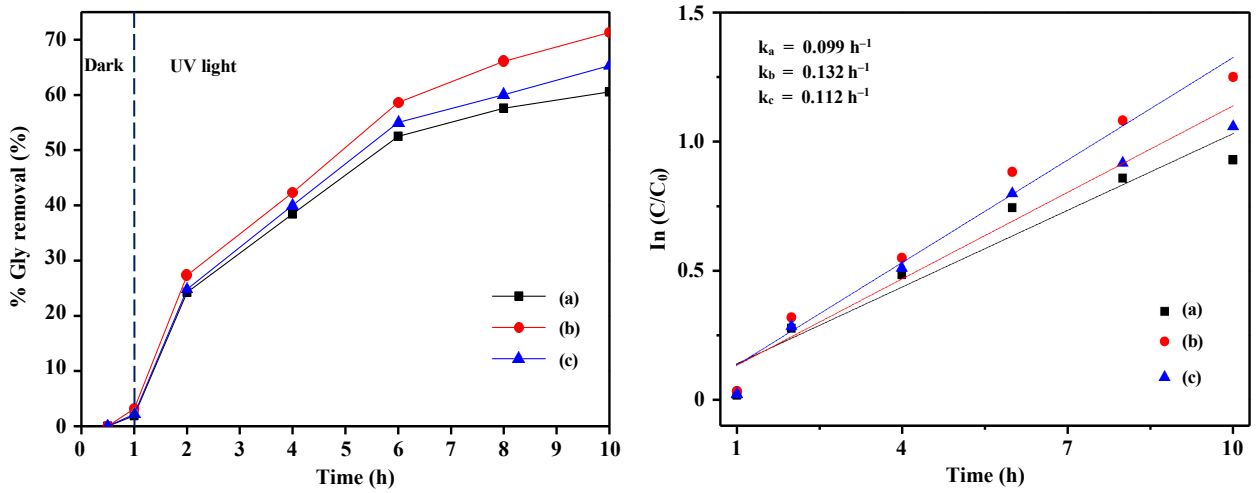

Figure 4. Removal rate of glyphosate as a function of UV light irradiation times and kinetic rate constant plot of CuO@NiO for different dosages at: (a) 3 mg, (b) 6 mg, and (c) 9 mg.

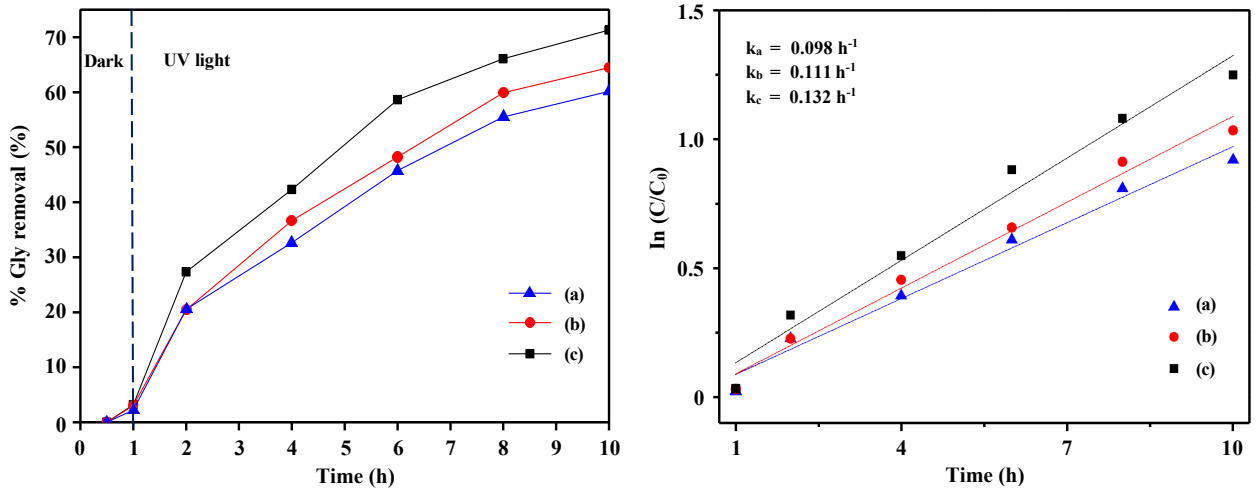

Figure 5. Removal rate of glyphosate as a function of UV light irradiation times and kinetic rate constant plot at 6 mg for different catalysts of: (a) NiO, (b) CuO, and (c) CuO@NiO.

Figure 5 shows the comparison of the removal Gly ability of CuO@NiO with pure NiO and CuO catalysts. At 6 mg of these catalysts were added to 25 mL Gly solution under UV light irradiation. The maximum degradation of Gly was obtained from CuO@NiO (71.23%), followed by CuO (64.46%) and NiO (60.17%), respectively. The results indicated the superiority and improvement in the photocatalytic activity of CuO@NiO over pure CuO and NiO. The reduced rate constant obtained from CuO@NiO to be 0.132 h^{-1}, was higher compared to the CuO to be 0.111 h^{-1}, and NiO to be 0.098 h^{-1}. The results were expected as it happened due to the synergetic effect between Cu and Ni.

4. Conclusions

CuO@NiO nanocomposite have been successfully developed and examined for the removal of glyphosate (Gly) solution. The material is a green catalytic, as the CuO@NiO was developed from mango (*Mangifera indica L.*) peel extracted solution. The morphology of CuO@NiO nanocomposite was observed to be subcluster, as the Ni cluster attached to the Cu cluster with a mean particle size of about 63.85 nm ± 1.26 nm. Pure CuO and NiO were also prepared by the same process. NiO was observed to be round with an average particle size of about 15.83 nm ± 0.58 nm, while CuO was obtained in a spherical shape with a bigger average particle size of about 33.74 nm ± 1.38 nm.

Experimental results showed that 6 mg of CuO@NiO nanocomposite showed high photocatalyst performance as capable of degrading Gly up to 71.23% and contained a kinetic value of about 0.132 h^{-1}. In addition, the use of CuO@NiO nanocomposite attained a high efficiency in the removal of Gly, which was higher than the value of pure CuO and NiO catalysts. The improvement and enhancement ability were derived from the synergetic effect of Cu and Ni. This work demonstrates an eco-friendly, low-cost material with high photodegradation of Gly solution for potential application in environmental protection.

Acknowledgements

The authors gratefully thank the Thailand Science Research and Innovation Fund. Contract No. FF66-P2-018 for financial support.

References

[1] M. Rodríguez Páez, Y. Ochoa-Muñoz, and J. E. Rodriguez-Páez, "Efficient removal of a glyphosate-based herbicide from water using ZnO nanoparticles (ZnO-NPs)," *Biocatalysis and Agricultural Biotechnology*, vol. 22, pp. 101434, 2019.

[2] M. Rani, and U. Shanker, "Degradation of traditional and new emerging pesticides in water by nanomaterials: recent trends and future recommendations," *International Journal of Environmental Science and Technology*, vol. 15, pp. 1347-1380, 2018.

[3] J. Z. Sandrini, R. C. Rola, F. M. Lopes, H. F. Buffon, M. M. Freitas, C. d. M. G. Martins, and C. E. Da Rosa, "Effects of glyphosate on cho-linesterase activity of the mussel Perna perna and the fish Danio rerio and Jenynsia multidentata: In vitro studies," *Aquatic Toxicology*, vol. 130, pp. 171-173, 2013.

[4] C. Feng, Y. Deng, L. Tang, G. Zeng, J. Wang, J. Yu, Y. Liu, B. Peng, H. Feng, and J. Wang, "Core-shell Ag_2CrO_4/N-GQDs @g-C_3N_4 composites with anti-photocorrosion performance for enhanced full-spectrum-light photocatalytic activities," *Applied Catalysis B: Environmental*, vol. 239, pp. 525-536, 2018.

[5] A. Zuorro, R. Lavecchia, M. M. Monaco, G. Iervolino, and V. Vaiano, "Photocatalytic degradation of azo dye reactive violet 5 on Fe-doped titania catalysts under visible light irradiation," *Catalysts*, vol. 9, p. 645, 2019.

[6] G. Iervolino, I. Zammit, V. Vaiano, and L. Rizzo, "Limitations and prospects for wastewater treatment by UV and Visi-ble-Light-Active heterogeneous photocatalysis: A critical review," *Topics in Current Chemistry*, vol. 7, p. 378, 2020.

[7] N. Tran, P. Drogui, T. L. Doan, T. S. Le, and H. C. Nguyen, "Electrochemical degradation and mineralization of glyphosate herbicide," *Environmental Technology*, vol 38. pp. 2939-2948, 2017.

[8] P. Marin, R. Bergamasco, A. N. Módenes, P. R. Paraiso, and S. Hamoudi, "Synthesis and characterization of graphene oxide functionalized with $MnFe_2O_4$ and supported on activated carbon for glyphosate adsorption in fixed bed column," *Process Safety and Environmental Protection*, vol. 123, pp. 59-71, 2019.

[9] C. A. Villamar-Ayala, J. V. Carrera-Cevallos, R. Vasquez-Medrano, and P. J. Espinoza-Montero, "Fate, eco-toxicological characteristics, and treatment processes applied to water polluted with glyphosate: A critical review," *Critical Reviews in Environmental Science and Technology*, vol. 49, pp. 1476-1514, 2019.

[10] R. K. Ibrahim, M. Hayyan, M. A. AlSaadi, A. Hayyan, and S. Ibrahim, "Environmental application of nanotechnology: Air, soil, and water," *Environmental Science and Pollution Research*, vol. 23, no. 14, pp. 13754-13788, 2016.

[11] K. D. Gilroy, A. Ruditskiy, H. -C. Peng, D. Qin, and Y. Xia, "Bimetallic nanocrystals: syntheses, properties, and applications," *Chemical Reviews*, vol. 116, no. 18, pp. 10414-10472, 2016.

[12] A. M. Alansi, M. A. Al-Qunaibit, I. O. Alade, T. F. Qahtan, and T. A. Saleh, "Visible- light responsive BiOBr nanoparticles loaded on reduced graphene oxide for photocatalytic degradation of dye," *Journal of Molecular Liquids*, vol. 253, pp. 297-304, 2018.

[13] N. N. Becknell, Y. Kang, C. Chen, J. Resasco, N. Kornienko, J. Guo, N. M. Markovic, G. A. Somorjai, V. R. Stamenkovic, and P. Yang, "Atomic structure of Pt_3Ni nonoframe electro-catalysts by in situ X-ray absorption spectroscopy," *Journal of the American Chemical Society*, vol. 137, pp. 15817-15824, 2015.

[14] Z. K. Ghouri, A. Badreldin, K. Elsaid, D. Kumar, K. Youssef, and A. Abdel-Wahab, "Theoretical and experimental investigations of Co-Cu bimetallic alloys-incorporated carbon nanowires as an efficient bi-functional electrocatalyst for water splitting," *Journal of Industrial and Engineering Chemistry*, vol. 96, pp. 243-253, 2021.

[15] N. Lee, and T. Hyeon, "Designed synthesis of uniformly sized iron oxide nanoparticles for efficient magnetic resonance imaging contrast agents," *Chemical Society Reviews*, vol. 41, pp. 2575-2589, 2012.

[16] L. M. Rossi, M. A. S. Garcia, and L. L. R. Vono, "Recent advances in the development of magnetically recoverable metal nanoparticle catalysts," *Journal of the Brazilian Chemical Society*, vol. 23, pp. 1959-1971, 2012.

[17] P. Srinoi, Y. T. Chen, V. Vittur, M. D. Marquez, and T. R. Lee, "Bimetallic nanoparticles: enhanced magnetic and optical properties for emerging biological applications," *Applied Sciences*, vol. 8, pp. 1-32, 2018.

[18] C. Y. Fu, K. W. Kho, U. S. Dinish, Z. Y. Koh, and O. Malini, "Enhancement in SERS intensity with hierarchical nano-structures by bimetallic deposition approach," *Journal of Raman Spectroscopy*, vol. 43, pp. 977-985, 2011.

[19] A. Baldi, T. C. Narayan, A. L. Koh, and J. A. Dionne, "In situ Detection of Hydrogen- Induced Phase Transitions in Individual Palladium Nanocrystals," *Nature Mater*, vol. 13, pp. 1143-1148, 2014.

[20] S. Medda, A. Hajra, U. Dey, P. Bose, and N. K. Mondal, "Biosynthesis of silver nanoparticles from Aloe vera leaf extract and antifungal activity against Rhizopus sp. and Aspergillus sp.," *Applied Nanoscience*, vol. 5, pp. 875-880, 2015.

[21] S. Mondal, N. Roy, R. A. Laskara, I. Sk, S. Basu, D. Mandal, and N. A. Begum, "Biogenic synthesis of Ag, Au and bimetallic Au/Ag alloy nanoparticles using aqueous extract of mahogany (Swietenia mahogani JACQ.) leaves," *Colloids and Surfaces B: Biointerfaces*, vol. 82, pp. 497-504, 2010.

[22] T. M. S. Rosbero, and D. H. Camacho, "Green preparation and characterization of tentacle-like silver/copper nanoparticles for catalytic degradation of toxic chlorpyrifos in water," *Journal of Environmental Chemical Engineering*, vol. 5, pp. 2524-2532, May. 2017.

[23] S. Kaviya, J. Santhanalakshmi, B. Viswanathan, J. Muthumary, and K. Srinivasan, "Biosynthesis of silver nanoparticles using citrus sinensis peel extract and its antibacterial activity," *Spectrochimica Acta Part A: Molecular and Biomolecular Spectroscopy*, vol. 79, pp. 594-598, 2011.

[24] Y. Xing, X. Liao, X. Liu, W. Li, R. Huang, J. Tang, Q. Xu, X. Li, and J. Yu, "characterization and antimicrobial activity of silver nanoparticles synthesized with the peel extract of mango," *Materials*, vol. 14, p. 5878, 2021.

[25] S. M. Roopan, A. Bharathi, R. Kumar, V. G. Khanna, and A. Prabhakarn, "Acaricidal, insecticidal, and larvicidal efficacy of aqueous extract of Annona squamosa L peel as biomaterial for the reduction of palladium salts into nanoparticles," *Colloids Surf B Biointerfaces*, vol. 1, pp. 209-212, 2012.

[26] R. K. Das, V. L. Pachapur, L. Lonappan, M. Naghdi, R. Pulicharla, S. Maiti, M. Cledón, L. M. A. Dalila, S. J. Sarma, and S. K. Brar, "Biological synthesis of metallic nanoparticles: Plants, animals and microbial aspects," *Nanotechnology for Environmental Engineering*, vol. 2, pp. 1-21, 2017.

[27] J. Singh, T. Dutta, K. H. Kim, M. Rawat, P. Samddar, and P. Kumar, "Green synthesis of metals and their oxide nanoparticles: Applications for environmental remediation," *Journal of Nanobiotechnology*, vol. 16, pp. 1-24, 2018.

[28] P. K. Dikshit, J. Kumar, A. K. Das, S. Sadhu, S. Sharma, S. Singh, P. K. Gupta, and B. S. Kim, "Green synthesis of metallic nanoparticles: Applications and limitations," *Catalysts*, vol. 11, pp. 1-35, 2021.

[29] N. K. Ojha, G. V. Zyryanov, A. Majee, V. N. Charushin, O. N. Chupakhin, and S. Santra, "Copper nanoparticles as inexpensive and efficient catalyst: a valuable contribution in organic synthesis," *Coordination Chemistry Reviews*, vol. 353, pp. 1- 57, 2017.

[30] L. Chen, H. Xu, H. Cui, H. Zhou, H. Wan, and J. Chen, "Preparation of Cu–Ni bimetallic nanoparticles surface-capped with dodecanethiol and their tribological properties as lubricant additive," *Particuology*, vol. 34, pp. 89-96, 2017.

[31] S. A. Hashemizadeh, and M. Biglari, "Cu:Ni bimetallic nanoparticles: facile synthesis, characterization and its application in photodegradation of organic dyes," *Journal of Materials Science: Materials in Electronics*, vol. 29, pp. 13025-13031, 2018.

[32] A. G. Ramu, M. L. A. Kumari, M. S. Elshikh, H. H. Alkhamis, A. F. Alrefaei, and D. Choi, "A facile and green synthesis of CuO/NiO nanoparticles and their removal activity of toxic nitro compounds in aqueous medium," *Chemosphere*, vol. 271, pp. 129475, 2021.

[33] U. Younas, A. Gulzar, F. Ali, M. Pervaiz, Z. Ali, S. Khan, Z. Saeed, M. Ahmed, and A. A. Alothman, "Antioxidant and organic dye removal potential of Cu-Ni bimetallic nanoparticles synthesized using gazania rigens extract," *Water*, vol. 13, p. 2653, 2021.

[34] Abdullah, T. Hussain, S. Faisal, M. Rizwan, S. N. Zaman, M. Iqbal, A. Iqbal, and Z. Ali, "Green synthesis and characterization of copper and nickel hybrid nanomaterials: Investigation of their biological and photocatalytic potential for the removal of organic crystal violet dye," *Journal of Saudi Chemical Society*, vol. 26, p. 101486, 2022.